

Hydroxy- and Mercaptopyridine Pincer Platinum and Palladium Complexes Generated by Silver-Free Halide Abstraction

Alexey V. Chuchuryukin,[†] Preston A. Chase,[†] Allison M. Mills,[‡] Martin Lutz,[‡] Anthony L. Spek,^{*,§} Gerard P. M. van Klink,[†] and Gerard van Koten^{*,†}

Debye Institute, Organic Chemistry and Catalysis, and Bijvoet Center for Biomolecular Research, Crystal and Structural Chemistry, Utrecht University, Padualaan 8, 3584 CH Utrecht, The Netherlands

Received October 13, 2005

A silver-free route has been employed for the synthesis of a number of Pd and Pt complexes supported by an NCN "pincer" ligand (NCN = [2,6-(Me₂NCH₂)₂C₆H₃]⁻) via halide abstraction. This was achieved by the use of *o*-, *m*-, and *p*-hydroxypyridines or *o*- and *p*-mercaptopyridines in basic ethanol solutions. The acidic OH or SH protons are removed to generate the formally anionic ligands. X-ray crystal structure determination of these complexes shows that the bonding of the substituted pyridine ligands occurs exclusively through the pyridine N for hydroxypyridines and exclusively through the thiol S in mercaptopyridines. In the hydroxypyridine case, the ortho and para isomers tautomerize to generate pyridone structures with a covalent M–N bond, whereas the *m*-hydroxypyridine complex, which is unable to tautomerize, is found to still be bound through the pyridine N but in a zwitterionic structure. The mercaptopyridine complexes are the first reported examples of pincer-ligated Pd and Pt thiolate species. The pyridine ligands can be quantitatively exchanged for chloride by reaction with excess NH₄Cl, a potentially useful chemical switch for ligation/decomplexation of this ligand type.

Introduction

The chemistry and application of transition-metal complexes containing the potentially terdentate monoanionic ECE pincer ligand (where pincer = [2,6-(ECH₂)₂C₆H₃]⁻; E = NR₂, PR₂, OR, SR, SeR) has been extensively explored.¹ These species have been used in such diverse fields as catalysis and small molecule activation,² polymer and dendrimer chemistry,^{3,4} and in selective sensing applications.⁵ Variation of the ligating group E allows for direct and simple modulation of the steric and electronic environment about the complexed metal center, whereas remote control of the electronic properties can be achieved by introduction of groups in the para position of the pincer arene.⁶ Because of the terdentate coordination of the pincer ligand, the organometallic M–C bond in the pincer systems are generally quite

robust, allowing, for instance, selective lithiation or nitration of the metal-bound aryl ring⁷ and use in high-temperature

- (2) Selected recent applications of pincer complexes: (a) Sebelius, S.; Ollson, V. J.; Szabó, K. J. *J. Am. Chem. Soc.* **2005**, *127*, 10478. (b) Kjellgren, J.; Sundén, H.; Szabó, K. J. *J. Am. Chem. Soc.* **2005**, *127*, 1787. (c) Solin, N.; Wallner, O. A.; Szabó, K. J. *Org. Lett.* **2005**, *7*, 689. (d) Solin, N.; Kjellgren, J.; Szabó, K. J. *J. Am. Chem. Soc.* **2004**, *126*, 7026. (e) Kjellgren, J.; Sundén, H.; Szabó, K. J. *J. Am. Chem. Soc.* **2004**, *126*, 474. (f) Wallner, O. A.; Szabó, K. J. *Org. Lett.* **2004**, *6*, 1829. (g) Solin, N.; Kjellgren, J.; Szabó, K. J. *Angew. Chem., Int. Ed.* **2003**, *42*, 3656. (h) Göttker-Schnetmann, I.; Brookhart, M. *J. Am. Chem. Soc.* **2004**, *126*, 9330. (i) Göttker-Schnetmann, I.; White, P.; Brookhart, M. *J. Am. Chem. Soc.* **2004**, *126*, 1804. (j) Göttker-Schnetmann, I.; White, P.; Brookhart, M. *Organometallics* **2004**, *23*, 1766. (k) Zhao, J.; Goldman, A. S.; Hartwig, J. F. *Science* **2005**, *307*, 1080. (l) Zhang, X.; Emge, T. J.; Ghosh, R.; Goldman, A. S. *J. Am. Chem. Soc.* **2005**, *127*, 8250. (m) Kanzelberger, M.; Zhang, X.; Emge, T. J.; Goldman, A. S.; Zhao, J.; Incarvito, C.; Hartwig, J. F. *J. Am. Chem. Soc.* **2003**, *125*, 13644. (n) Kanzelberger, M.; Singh, B.; Czerw, M.; Krogh-Jespersen, K.; Goldman, A. S. *J. Am. Chem. Soc.* **2000**, *122*, 11017. (o) Amoroso, D.; Jabri, A.; Yap, G. P. A.; Gusev, D. G.; dos Santos, E. N.; Fogg, D. E. *Organometallics* **2004**, *23*, 4047. (p) Gagliardo, M.; Dijkstra, H. P.; Coppo, P.; De Cola, L.; Lutz, M.; Spek, A. L.; van Klink, G. P. M.; van Koten, G. *Organometallics* **2004**, *23*, 5833. (q) Eberhard, M. R. *Org. Lett.* **2004**, *6*, 2125. (r) Yao, Q.; Kinney, E. P.; Zheng, Z. *Org. Lett.* **2004**, *6*, 2997. (s) Cohen, R.; Milstein, D.; Martin, J. M. L. *Organometallics* **2004**, *23*, 2342. (t) Kozhanov, K. A.; Bobnov, M. P.; Cherkasov, V. K.; Fukin, G. K.; Abakumov, G. A. *Dalton Trans.* **2004**, 2957. (u) Morales-Morales, D.; Redon, R.; Yung, C.; Jensen, C. *Inorg. Chim. Acta* **2004**, *357*, 2953. (v) Chase, P. A.; Gagliardo, M.; van Klink, G. P. M.; Lutz, M.; Spek, A. L.; van Koten, G. *Organometallics* **2005**, *24*, 2016. (w) Kossov, E.; Iron, M. A.; Rybtchinski, B.; Ben-David, Y.; Shimon, L. J. W.; Konstantinovskii, L.; Martin, J. M. L.; Milstein, D. *Chem.—Eur. J.* **2005**, *11*, 2321.

* To whom correspondence should be addressed. Tel: 31-30-253-3120. Fax: 31-30-252-3615. E-mail: g.vankoten@chem.uu.nl.

[†] Debye Institute.

[‡] Bijvoet Center for Biomolecular Research, Crystal and Structural Chemistry.

[§] Corresponding author for crystallographic inquiries. E-mail: a.l.spek@chem.uu.nl.

(1) For recent reviews see: (a) Albrecht, M.; van Koten, G. *Angew. Chem., Int. Ed.* **2001**, *41*, 3750. (b) van der Boom, M. E.; Milstein, D. *Chem. Rev.* **2003**, *103*, 1759. (c) Templeton, J. T. *Tetrahedron* **2003**, *59*, 1837. (d) Jensen, C. M. *Chem. Commun.* **1999**, 2443. (e) Gossage, R. A.; van de Kuil, L. A.; van Koten, G. *Acc. Chem. Res.* **1998**, *31*, 423.

catalytic processes, such as PCP–Ir-catalyzed alkane dehydrogenation.^{1d,2h–j}

For group 10 metals (Ni, Pd, Pt), the common starting material for exploration of the aforementioned applications is generally the ECE–M halides. A common route to remove halides from mid-to-late transition-metal complexes is achieved via Ag⁺-mediated reactions,⁸ and the subsequent metal cations generated are generally considered to be more reactive than the parent halides.⁹ Indeed, this is the preferred method for the synthesis of a number of pincer-supported group 10 metal cations, which have been employed as Lewis acid catalysts in Michael addition chemistry¹⁰ and, recently, to probe dynamic control of the properties of supramolecular polymers and networks.¹¹ The insolubility of the AgX salts is the driving force for this reaction. However, there are some technical difficulties associated with the employment of silver reagents. Besides their relatively high cost, they are also quite

light sensitive and very hygroscopic. As such, alternative, silver-free routes would be desirable. In NCN pincer Pt iodide complexes, it was previously found that the addition of polar, coordinating dimethylformamide (DMF) establishes an equilibrium in which there is partial displacement of the covalently bound iodide by a molecule of solvent, generating an ion pair.¹² The outer sphere iodide anion can then be exchanged for perchlorate (ClO₄[−]) on an ion-exchange resin. We reasoned that alternate chemical reagents could be employed to force this equilibrium toward the ion-separated or halide-abstracted products.

In addition to the previously mentioned technical problems related to the use of silver reagents, trace amounts of silver can remain in the products and potentially interfere with subsequent reactions. Silver complexes and salts are very active catalysts for a number of reactions,¹³ and trace amounts could potentially interfere in catalyst screening. Also, multimetallic pyridine complexes of NCN–Pt and NCN–Pd pincers have recently been employed as templates for the generation of poly(pyridine) macroheterocycles via ring-closing metathesis.¹⁴ In the synthesis of macroheterocycles containing polyether linkages between the pyridine groups, up to 10% of the generated silver halide was sequestered and solubilized by the “crownlike” polyethers.¹⁵ The residual silver was found to interfere with the subsequent metathesis reactions, which necessitated removal by reaction with highly toxic H₂S.^{14a,b} Here, we report a silver-free synthetic route for the synthesis of a number of Pt and Pd NCN pincer (NCN = [2,6-(Me₂NCH₂)₂C₆H₃][−]) complexes containing hydroxy-

- (3) (a) Knapen, J. W. J.; van der Made, A. W.; De Wilde, J. C.; van Leeuwen, P. W. N. M.; Wijkens, P.; Grove, D. M.; van Koten, G. *Nature* **1994**, *372*, 659. (b) Kleij, A. W.; Gossage, R. A.; Jastrzebski, J. T. B. H.; Boersma, J.; van Koten, G. *Angew. Chem., Int. Ed.* **2000**, *39*, 176. (c) Kleij, A. W.; Gossage, R. A.; Klein Gebbink, R. J. M.; Brinkmann, N.; Reijerse, E. J.; Kragl, U.; Lutz, M.; Spek, A. L.; van Koten, G. *J. Am. Chem. Soc.* **2000**, *122*, 12112. (d) Albrecht, M.; Hovestad, N. J.; Boersma, J.; van Koten, G. *Chem.–Eur. J.* **2001**, *7*, 1289. (e) Dahan, A.; Weissberg, A.; Portnoy, M. *Chem. Commun.* **2003**, 1206. (f) Chase, P. A.; Klein Gebbink, R. J. M.; van Koten, G. *J. Organomet. Chem.* **2004**, *689*, 4016.
- (4) (a) Huck, W. T. S.; van Veggel, F. C. J. M.; Reinhoudt, D. N. *Angew. Chem., Int. Ed.* **1996**, *35*, 1213. (b) Huck, W. T. S.; Hulst, R.; Timmerman, P.; van Veggel, F. C. J. M.; Reinhoudt, D. N. *Angew. Chem., Int. Ed.* **1997**, *36*, 1006. (c) Huck, W. T. S.; van Veggel, F. C. J. M.; Reinhoudt, D. N. *New J. Chem.* **1998**, *22*, 165. (d) van Manen, H.-J.; Fokkens, R. H.; van Veggel, F. C. J. M.; Reinhoudt, D. N. *Eur. J. Org. Chem.* **2002**, *18*, 3189. (e) van Manen, H.-J.; van Veggel, F. C. J. M.; Reinhoudt, D. N. *Top. Curr. Chem.* **2001**, *217*, 121. (f) van de Coevering, R.; Kuil, M.; Klein Gebbink, R. J. M.; van Koten, G. *Chem. Commun.* **2002**, 1636.
- (5) (a) Albrecht, M.; Lutz, M.; Spek, A. L.; van Koten, G. *Nature* **2000**, *406*, 970. (b) Albrecht, M.; Schlupp, M.; Bargon, J.; van Koten, G. *Chem. Commun.* **2001**, 1874. (c) Robitzer, M.; Sirlin, C.; Kyritsakas, N.; Pfeffer, M. *Eur. J. Inorg. Chem.* **2002**, 2312. (d) Robitzer, M.; Bouamäed, I.; Sirlin, C.; Chase, P. A.; van Koten, G.; Pfeffer, M. *Organometallics* **2005**, *24*, 1756.
- (6) (a) van de Kuil, L. A.; Luitjes, H.; Grove, D. M.; Zwikker, J. W.; van der Linden, J. G. M.; Roelofsen, A. M.; Jenneskens, L. W.; Drenth, W.; van Koten, G. *Organometallics* **1994**, *13*, 468. (b) Dijkstra, H. P.; Slagt, M. Q.; McDonald, A.; Kruithof, C. A.; Kreiter, R.; Mills, A. M.; Lutz, M.; Spek, A. L.; Klopper, W.; van Klink, G. P. M.; van Koten, G. *Eur. J. Inorg. Chem.* **2003**, 830. (c) Slagt, M. Q.; Rodríguez, G.; Grutters, M. M. P.; Klein Gebbink, R. J. M.; Klopper, W.; Jenneskens, L. W.; Lutz, M.; Spek, A. L.; van Koten, G. *Chem.–Eur. J.* **2004**, 1331.
- (7) Rodríguez, G.; Albrecht, M.; Schoenmaker, J.; Ford, A.; Lutz, M.; Spek, A. L.; van Koten, G. *J. Am. Chem. Soc.* **2002**, *124*, 5127.
- (8) (a) Liston, D. J.; Lee, Y. J.; Scheidt, W. R.; Reed, C. A. *J. Am. Chem. Soc.* **1989**, *111*, 6643. (b) Albano, V. G.; Di Serio, M.; Monari, M.; Orabona, I.; Panunzi, A.; Ruffo, F. *Inorg. Chem.* **2002**, *41*, 2672.
- (9) For examples see: (a) Ittel, S. D.; Johnson, L. K.; Brookhart, M. *Chem. Rev.* **2000**, *100*, 1169. (b) Hahn, C.; Morvillo, P.; Vitagliano, A. *Eur. J. Inorg. Chem.* **2001**, 419.
- (10) For recent examples see: (a) Slagt, M. Q.; van Zwieten, D. A. P.; Moerkerk, A. J. C. M.; Klein Gebbink, R. J. M.; van Koten, G. *Coord. Chem. Rev.* **2004**, *248*, 2275. (b) Takenaka, K.; Uozumi, Y. *Org. Lett.* **2004**, *6*, 1833. (c) Takenaka, K.; Minakawa, M.; Uozumi, Y. *J. Am. Chem. Soc.* **2005**, *127*, 12273. (d) Fossey, J. S.; Richards, C. J. *J. Organomet. Chem.* **2004**, *689*, 3056. (e) Fossey, J. S.; Richards, C. J. *Organometallics* **2004**, *23*, 367. (f) Dijkstra, H. P.; Meijer, M. D.; Patel, J.; Kreiter, R.; van Klink, G. P. M.; Lutz, M.; Spek, A. L.; Cauty, A. J.; van Koten, G. *Organometallics* **2001**, *20*, 3159–3168.
- (11) (a) Yount, W. C.; Juwarker, H.; Craig, S. L. *J. Am. Chem. Soc.* **2003**, *125*, 15302. (b) Yount, W. C.; Loveless, D. M.; Craig, S. L. *Angew. Chem., Int. Ed.* **2005**, *44*, 2746.
- (12) Schmülling, M.; Grove, D. M.; van Koten, G.; van Eldik, R.; Veldman, N.; Spek, A. L. *Organometallics* **1996**, *15*, 1384.
- (13) Some selected examples: (a) Yanagisawa, A.; Touge, T.; Arai, T. *Angew. Chem., Int. Ed.* **2005**, *44*, 1546. (b) Wadamoto, M.; Ozasa, N.; Yanagisawa, A.; Yamamoto, H. *J. Org. Chem.* **2003**, *68*, 5593. (c) Yanagisawa, A.; Matsumoto, Y.; Asakawa, K.; Yamamoto, H. *Tetrahedron* **2002**, *58*, 8331. (d) Yanagisawa, A.; Nakatsuka, Y.; Asakawa, K.; Wadamoto, M.; Kageyama, H.; Yamamoto, H. *Bull. Chem. Soc. Jpn.* **2001**, *74*, 1477. (e) Rhee, J. U.; Kriscic, M. J. *Org. Lett.* **2005**, *7*, 2493. (f) Cesarotti, E.; Araneo, S.; Rimoldi, I.; Tassi, S. *J. Mol. Catal. A: Chem.* **2003**, *204–205*, 221. (g) Jiang, N.; Ma, Z.; Qu, Z.; Xing, X.; Xie, L.; Wang, J. *J. Org. Chem.* **2003**, *68*, 893. (h) Patmore, N. J.; Hague, C.; Cotgreave, J. H.; Mahon, M. F.; Frost, C. G.; Weller, A. S. *Chem.–Eur. J.* **2002**, *8*, 2088. (i) Crist, D. R.; Hsieh, Z. H.; Quicksall, C. O.; Sun, M. K. *J. Org. Chem.* **1984**, *49*, 2478. (j) Yanagisawa, A. In *Modern Aldol Reactions*; Mahrwald, R., Ed.; Wiley-VCH: Weinheim, Germany, 2004; p 1. (k) Yanagisawa, A. In *Lewis Acids in Organic Synthesis*; Yamamoto, H., Ed.; Wiley-VCH: Weinheim, Germany, 2000; Vol. 2, p 575. (l) Sawamura, M. In *Lewis Acid Reagents*; Yamamoto, H., Ed.; Oxford University Press: Oxford, U.K., 1999; p 169.
- (14) (a) Chuchuryukin, A. V.; Chase, P. A.; Dijkstra, H. P.; Suijkerbuijk, B. M. J. M.; van Klink, G. P. M.; Mills, A. M.; Spek, A. L.; van Koten, G. *Adv. Synth. Catal.* **2005**, *347*, 447. (b) Chuchuryukin, A. V.; Dijkstra, H. P.; Suijkerbuijk, B. M. J. M.; van Klink, G. P. M.; Klein Gebbink, R. J. M.; Mills, A. M.; Spek, A. L.; van Koten, G. *Russ. J. Org. Chem.* **2003**, *39*, 422. (c) Chuchuryukin, A. V.; Dijkstra, H. P.; Suijkerbuijk, B. M. J. M.; van Klink, G. P. M.; Klein Gebbink, R. J. M.; Mills, A. M.; Spek, A. L.; van Koten, G. *Angew. Chem., Int. Ed.* **2003**, *42*, 228. (d) Dijkstra, H. P.; Chuchuryukin, A. V.; Suijkerbuijk, B. M. J. M.; van Klink, G. P. M.; Mills, A. M.; Spek, A. L.; van Koten, G. *Adv. Synth. Catal.* **2002**, *344*, 771. (e) For a review see: Chase, P. A.; Lutz, M.; Spek, A. L.; van Klink, G. P. M.; van Koten, G. *J. Mol. Catal. A: Chem.* **2005**, submitted for publication.
- (15) (a) Inoue, Y.; Gokel, G. W. *Cation Binding by Macrocycles*; Marcel Dekker: New York, 1990. (b) Pedersen, C. J. *J. Am. Chem. Soc.* **1967**, *89*, 7017–7036. (c) Newkome, G. R.; Marston, C. R. *Tetrahedron* **1983**, *39*, 2001–2008. (d) Weber, E.; Vögtle, F. *Angew. Chem., Int. Ed.* **1980**, *19*, 1030–1032.

and mercaptopyridine ligands and analysis of the binding mode of the heteroatom-substituted pyridine ligands via X-ray crystallography.

Experimental Section

All reactions were carried out using standard Schlenk techniques under an inert atmosphere of dry, oxygen-free nitrogen unless stated otherwise. All solvents were dried and distilled under N₂ prior to use. Ethanol was dried with Na, diethyl ether over Na/benzophenone, CH₂Cl₂ over CaH₂, and pentane over Na metal. Pincer compounds NCN–PdCl¹⁶ and NCN–PtCl¹⁷ were synthesized via literature procedures, and all other standard reagents were purchased from Acros or Aldrich and used as received. ¹H (300 MHz) and ¹³C (75 MHz) NMR spectra were recorded on a Varian Inova 300 MHz spectrometer and chemical shifts (δ) are given in ppm and referenced to residual solvent signals. Elemental analyses were performed by H. Kolbe Microanalytical Laboratories, Mülheim an der Ruhr, Germany.

[2,6-Bis(dimethylaminomethyl)phenylplatinum]-2-pyridone (3a). Pincer complex NCN–PtCl (**1**) (137 mg, 0.32 mmol), 2-hydroxypyridine (31 mg, 0.33 mmol), and sodium hydroxide (20 mg, 0.5 mmol) were weighed into a small Schlenk flask and placed under N₂. Ethanol (5 mL) was added via syringe, and the reaction was stirred for 2 h. Solvent was evaporated in vacuo. The residues were redissolved in air in dichloromethane (10 mL) and filtered. Filtrate was evaporated in vacuo to obtain **3a** as a white solid. Yield: 150 mg (96%). X-ray quality crystals were obtained by vapor diffusion of diethyl ether into a saturated CH₂Cl₂ solution of **3a**.

¹H NMR (300 MHz, CDCl₃): δ 2.6–3.2 (bs, 12H, NMe₂), 4.06 (t, ³J_{H–Pt} = 24.1 Hz, 4H, CH₂N), 6.14 (td, ³J_{H–H} = 6.2 Hz, ⁴J_{H–H} = 1.1 Hz, 1H, CH), 6.45 (d, ³J_{H–H} = 8.8 Hz, 2H, CHCO), 6.83 (d, ³J_{H–H} = 7.3 Hz, 2H, ArH), 6.98 (t, ³J_{H–H} = 7.5 Hz, 1H, ArH), 7.19 (td, ³J_{H–H} = 7.7 Hz, ⁴J_{H–H} = 2.2 Hz, 1H, CH), 7.77 (dd, ³J_{H–H} = 6.0 Hz, ⁴J_{H–H} = 2.3 Hz, 1H, CHN). ¹³C NMR (75 MHz, CDCl₃): δ 54.2, 78.0, 106.6, 119.1, 119.2, 123.5, 137.0, 144.4, 146.7, 149.2, 171.4. Anal. Calcd for C₁₇H₂₃N₃OPt: C, 42.50; H, 4.83; N, 8.75. Found: C, 42.64; H, 4.76; N, 8.83.

[2,6-Bis(dimethylaminomethyl)phenylpalladium]-2-pyridone (3b). Synthesis was performed in a method analogous to that for **3a** using NCN–PdCl (**2**) (100 mg, 0.30 mmol), 2-hydroxypyridine (29 mg, 0.30 mmol), and sodium hydroxide (17 mg, 0.43 mmol). Yield: 66 mg (56%). X-ray quality crystals were obtained by vapor diffusion of pentane into a saturated CH₂Cl₂ solution of **3b**.

¹H NMR (300 MHz, CDCl₃): δ 2.78 (s, 12H, NMe₂), 4.00 (s, 4H, CH₂N), 6.08 (td, ³J_{H–H} = 6.2 Hz, ⁴J_{H–H} = 0.9 Hz, 1H, CH), 6.38 (d, ³J_{H–H} = 9.0 Hz, 2H, CHCO), 6.78 (d, ³J_{H–H} = 7.2 Hz, 2H, ArH), 6.95 (t, ³J_{H–H} = 7.5 Hz, 1H, ArH), 7.17 (ddd, ³J_{H–H} = 8.7 Hz, ³J_{H–H} = 6.6 Hz, ⁴J_{H–H} = 2.1 Hz, 1H, CH), 7.73 (dd, ³J_{H–H} = 5.6 Hz, ⁴J_{H–H} = 2.0 Hz, 1H, CHN). ¹³C NMR (75 MHz, CDCl₃): δ 52.7, 75.0, 106.4, 117.8, 119.7, 124.5, 137.2, 145.5, 146.2, 158.9, 171.9. Anal. Calcd for C₁₇H₂₃N₃OPd: C, 52.11; H, 5.92; N, 10.72. Found: C, 52.04; H, 6.12; N, 10.65.

[2,6-Bis(dimethylaminomethyl)phenylplatinum]-4-pyridone (4a). Synthesis was performed in a method analogous to that for **3a** using NCN–PtCl (**1**) (160 mg, 0.38 mmol), 4-hydroxypyridine (36 mg, 0.38 mmol), and sodium hydroxide (20 mg, 0.50 mmol).

Yield: 182 mg (99%). X-ray quality crystals were obtained by vapor diffusion of diethyl ether into a saturated CH₂Cl₂ solution of **4a**.

¹H NMR (300 MHz, CDCl₃): δ 2.83 (t, ³J_{H–Pt} = 19.7 Hz, 12H, NMe₂), 4.12 (t, ³J_{H–Pt} = 23.6 Hz, 4H, CH₂N), 6.51 (d, ³J_{H–H} = 7.0 Hz, 2H, CHCO), 6.87 (d, ³J_{H–H} = 7.9 Hz, 2H, ArH), 7.02 (t, ³J_{H–H} = 7.5 Hz, 1H, ArH), 7.75 (d, ³J_{H–H} = 7.0 Hz, 2H, CHN). ¹³C NMR (75 MHz, CDCl₃): δ 54.1, 78.2, 119.5, 119.6, 124.6, 144.5, 146.6, 148.2, 178.1. Anal. Calcd for C₁₇H₂₃N₃OPt: C, 42.50; H, 4.83; N, 8.75. Found: C, 42.38; H, 4.92; N, 8.67.

[2,6-Bis(dimethylaminomethyl)phenylpalladium]-4-pyridone (4b). Synthesis was performed in a method analogous to that for **3a** using NCN–PdCl (**2**) (100 mg, 0.30 mmol), 4-hydroxypyridine (30 mg, 0.32 mmol), and sodium hydroxide (17 mg, 0.43 mmol). Yield: 62 mg (53%). X-ray quality crystals were obtained by vapor diffusion of water into a saturated acetone solution of **4b** in the air.

¹H NMR (300 MHz, CDCl₃): δ 2.69 (s, 12H, NMe₂), 4.05 (s, 4H, CH₂N), 6.51 (d, ³J_{H–H} = 6.9 Hz, 2H, CHCO), 6.82 (d, ³J_{H–H} = 7.5 Hz, 2H, ArH), 7.02 (t, ³J_{H–H} = 7.5 Hz, 1H, ArH), 7.77 (d, ³J_{H–H} = 6.6 Hz, 2H, CHN). ¹³C NMR (75 MHz, CDCl₃): δ 52.7, 75.2, 119.2, 120.2, 125.5, 145.4, 148.0, 156.9, 178.1. Anal. Calcd for C₁₇H₂₃N₃OPd: C, 52.11; H, 5.92; N, 10.72. Found: C, 51.97; H, 6.00; N, 10.65.

[2,6-Bis(dimethylaminomethyl)phenylplatinum]-3-pyridineoxide (5). Synthesis was performed in a method analogous to that of **3a** using NCN–PtCl (**1**) (137 mg, 0.32 mmol), 3-hydroxypyridine (35 mg, 0.37 mmol), and sodium hydroxide (20 mg, 0.50 mmol). Yield: 85 mg (54%). Crystals were obtained by the slow evaporation of a saturated, wet 2-propanol solution of **5** in the air.

¹H NMR (300 MHz, CD₃OD): δ 2.82 (td, ³J_{H–Pt} = 19.7 Hz, ³J_{H–H} = 5.1 Hz, 12H, NMe₂), 4.19 (t, ³J_{H–Pt} = 24 Hz, 4H, CH₂N), 6.90 (d, ³J_{H–H} = 7.2 Hz, 2H, ArH), 7.02 (dd, ³J_{H–H} = 8.1 Hz, ³J_{H–H} = 6.6 Hz, 1H, ArH), 7.07 (dq, ³J_{H–H} = 8.7 Hz, ⁴J_{H–H} = 1.4 Hz, 1H, CHCO), 7.29 (dd, ³J_{H–H} = 8.6 Hz, ³J_{H–H} = 5.0 Hz, 1H, CH), 7.94 (dd, ³J_{H–H} = 5.3 Hz, ⁴J_{H–H} = 1.1 Hz, 1H, CHN), 8.13 (d, ⁴J_{H–H} = 2.7 Hz, 1H, CHN). ¹³C NMR (75 MHz, CD₃OD): δ 54.0, 78.5, 120.3, 125.9, 127.9, 128.5, 136.8, 143.8, 145.5, 146.0, 167.1. Anal. Calcd for C₁₇H₂₃N₃OPt: C, 42.50; H, 4.83; N, 8.75. Found: C, 42.46; H, 4.76; N, 8.67.

[2,6-Bis(dimethylaminomethyl)phenylplatinum]-4-thiolatopyridine (6a). Synthesis was performed in a method analogous to that for **3a** using NCN–PtCl (**1**) (56 mg, 0.13 mmol), 4-mercaptopyridine (15 mg, 0.13 mmol), and sodium hydroxide (9 mg, 0.23 mmol). Yield: 63 mg (96%). X-ray quality crystals were obtained by vapor diffusion of diethyl ether into a saturated CH₂Cl₂ solution of **6a**.

¹H NMR (300 MHz, CDCl₃): δ 3.07 (t, ³J_{H–Pt} = 19.7 Hz, 12H, NMe₂), 4.12 (t, ³J_{H–Pt} = 22.5 Hz, 4H, CH₂N), 6.91 (d, ³J_{H–H} = 7.5 Hz, 2H, ArH), 7.06 (dd, ³J_{H–H} = 8.0 Hz, ³J_{H–H} = 7.0 Hz, 1H, ArH), 7.75 (dd, ³J_{H–H} = 4.8 Hz, ⁴J_{H–H} = 1.5 Hz, 2H, CHCS), 8.07 (dd, ³J_{H–H} = 4.5 Hz, ⁴J_{H–H} = 1.5 Hz, 2H, CHN). ¹³C NMR (75 MHz, CDCl₃): δ 54.9, 79.3, 119.3, 124.5, 127.3, 144.2, 147.7, 155.3, 163.0. Anal. Calcd for C₁₇H₂₃N₃PtS: C, 41.12; H, 4.67; N, 8.46. Found: C, 41.04; H, 4.67; N, 8.37.

[2,6-Bis(dimethylaminomethyl)phenylpalladium]-4-thiolatopyridine (6b). Synthesis was performed in a method analogous to that for **3a** using NCN–PdCl (**2**) (100 mg, 0.30 mmol), 4-mercaptopyridine (34 mg, 0.31 mmol), and sodium hydroxide (15 mg, 0.38 mmol). Yield: 55 mg (45%). X-ray quality crystals were obtained by vapor diffusion of pentane into a saturated CH₂Cl₂ solution of **6b**.

¹H NMR (300 MHz, CDCl₃): δ 2.90 (s, 12H, NMe₂), 4.06 (s, 4H, CH₂N), 6.83 (d, ³J_{H–H} = 7.2 Hz, 2H, ArH), 7.02 (t, ³J_{H–H} =

(16) Alsters, P. L.; Baesjou, P. J.; Janssen, M. D.; Kooijman, H.; Sicherer-Roetman, A.; Spek, A. L.; van Koten, G. *Organometallics* **1992**, *11*, 4124.

(17) Grove, D. M.; van Koten, G.; Louwen, J. N.; Noltes, J. G.; Spek, A. L.; Ubbels, H. J. C. *J. Am. Chem. Soc.* **1982**, *104*, 6609.

Table 1. Experimental Crystallographic Details for **3a**, **3b**, **4a**, and **4b**

	3a	3b	4a	4b
formula	C ₁₇ H ₂₃ N ₃ OPt·CH ₂ Cl ₂	C ₁₇ H ₂₃ N ₃ OPd	C ₁₇ H ₂₃ N ₃ OPT·H ₂ O	C ₁₇ H ₂₃ N ₃ OPd·2.5H ₂ O
fw	565.40	391.78	498.49	436.82
cryst color	colorless	yellow	colorless	colorless
cryst size (mm ³)	0.15 × 0.12 × 0.06	0.24 × 0.24 × 0.06	0.42 × 0.05 × 0.03	0.60 × 0.15 × 0.12
cryst syst	monoclinic	monoclinic	monoclinic	triclinic
space group	<i>P</i> 2 ₁ / <i>c</i> (No. 14)	<i>P</i> 2 ₁ / <i>c</i> (No. 14)	<i>P</i> 2 ₁ / <i>c</i> (No. 14)	<i>P</i> 1̄ (No. 2)
<i>a</i> (Å)	11.5203(2)	8.5072(6)	10.0702(3)	8.9685(4)
<i>b</i> (Å)	13.0330(3)	15.7519(9)	18.2011(4)	10.3356(6)
<i>c</i> (Å)	16.9135(4)	13.1651(5)	9.8155(2)	20.2901(11)
α (deg)	90	90	90	85.786(5)
β (deg)	128.4340(13)	115.722(6)	90.7806(9)	87.660(4)
γ (deg)	90	90	90	88.475(4)
<i>V</i> (Å ³)	1989.22(8)	1589.37(18)	1798.90(8)	1873.61(17)
<i>Z</i>	4	4	4	4
<i>D</i> _{calcd} (g/cm ³)	1.888	1.637	1.841	1.549
μ (mm ⁻¹)	7.334	1.173	7.813	1.013
abs corr	DELABS (PLATON ²²)	SADABS ²³	DELABS (PLATON ²²)	SADABS ²³
abs corr range	0.38–0.64	0.70–0.93	0.40–0.80	0.75–0.89
(sin θ/λ) _{max} (Å ⁻¹)	0.65	0.65	0.65	0.65
no. of measured reflns	20343	27485	18573	40141
no. of unique reflns	4500	3644	4095	8598
params/restraints	230/0	218/33	218/1	480/15
R1/wR2 [<i>I</i> > 2σ(<i>I</i>)]	0.0279/0.0417	0.0210/0.0453	0.0343/0.0633	0.0202/0.0469
R1/wR2 (all reflns)	0.0509/0.0458	0.0298/0.0485	0.0604/0.0707	0.0266/0.0491
<i>S</i>	0.961	1.049	1.029	1.024
ρ _{min/max} (e Å ⁻³)	−0.68/1.06	−0.64/0.59	−1.24/1.34	−0.42/0.73

7.5 Hz, 1H, ArH), 7.69 (dd, ³*J*_{H–H} = 4.8 Hz, ⁴*J*_{H–H} = 1.8 Hz, 2H, CHCS), 8.05 (dd, ³*J*_{H–H} = 5.0 Hz, ⁴*J*_{H–H} = 1.7 Hz, 2H, CHN). ¹³C NMR (75 MHz, CDCl₃): δ 53.4, 76.1, 119.8, 125.2, 128.2, 145.4, 147.8, 161.7, 163.1. Anal. Calcd for C₁₇H₂₃N₃PdS·0.15CH₂Cl₂: C, 48.97; H, 5.58; N, 9.99. Found: C, 49.02; H, 5.38; N, 9.53.

[2,6-Bis(dimethylaminomethyl)phenylplatinum]-2-thiolatopyridine (7). Synthesis was performed in a method analogous to that for **3a** using NCN–PtCl (**1**) (56 mg, 0.13 mmol), 2-mercaptopyridine (15 mg, 0.13 mmol), and sodium hydroxide (9 mg, 0.23 mmol). Yield: 62 mg (94%). X-ray quality crystals were obtained by vapor diffusion of pentane into a saturated CH₂Cl₂ solution of **7**.

¹H NMR (300 MHz, CDCl₃): δ 3.11 (t, ³*J*_{H–Pt} = 19.9 Hz, 12H, NMe₂), 4.10 (t, ³*J*_{H–Pt} = 21.5 Hz, 4H, CH₂N), 6.70 (ddd, ³*J*_{H–H} = 7.1 Hz, ³*J*_{H–H} = 5.0 Hz, ⁴*J*_{H–H} = 0.9 Hz, 1H, CH), 6.89 (d, ³*J*_{H–H} = 7.5 Hz, 2H, ArH), 7.03 (t, ³*J*_{H–H} = 7.4 Hz, 1H, ArH), 7.22 (td, ³*J*_{H–H} = 7.7 Hz, ⁴*J*_{H–H} = 1.8 Hz, 1H, CH), 7.89 (d, ³*J*_{H–H} = 8.1 Hz, 2H, CHCS), 8.26 (dq, ³*J*_{H–H} = 5.0 Hz, ⁴*J*_{H–H} = 0.9 Hz, 1H, CHN). ¹³C NMR (75 MHz, CDCl₃): δ 54.9, 79.4, 115.9, 119.1, 124.0, 127.2, 134.1, 144.3, 149.0, 155.7, 172.7. Anal. Calcd for C₁₇H₂₃N₃PtS: C, 41.12; H, 4.67; N, 8.46. Found: C, 40.97; H, 4.72; N, 8.41.

X-ray Crystallographic Data. X-ray intensity data were collected on a Nonius KappaCCD diffractometer with rotating anode (graphite monochromator, λ = 0.71073 Å). The structures were solved with automated Patterson methods¹⁸ and refined with SHELXL-97¹⁹ against *F*² of all reflections. Non-hydrogen atoms were refined freely with anisotropic displacement parameters. The hydrogen atoms of the H₂O molecules of **4a** and **4b** were refined with isotropic displacement parameters (with OH distance and angle restraints); all other hydrogen atoms were refined with a riding model. In **4b**, there are only two oxygen atoms in proximity of O4: O3 and O2. O3 is a hydrogen bond donor with O4 as acceptor.

O4 is donating a hydrogen bond to O2 via hydrogen H4B. There is no hydrogen bond acceptor available for H4A. Hydrogen atom positions of H4A and H4B were confirmed in the difference Fourier map. One pincer arm of **3b** was refined with a disorder model. The crystals of the isostructural **6a** and **6b** appeared to be non-merohedrally twinned, with a 2-fold rotation about the reciprocal *b** axis as the twin operation. This twinning was taken into account during intensity evaluation,²⁰ data reduction, and structure refinement with the HKLF5²¹ option of SHELXL-97.¹⁹ The twinned crystal of **6a** was weakly diffracting up to a resolution of (sin θ/λ)_{max} = 0.53 Å⁻¹. An absorption correction for the twinned crystal of **6b** was considered unnecessary. Geometry calculations, structure validation, and molecular graphics were performed with the PLATON²² package. Further crystallographic details are given in Tables 1 and 2.

Results and Discussion

Synthesis of Complexes. Halide abstraction from NCN–PtCl (**1**) and NCN–PdCl (**2**) can be achieved simply in basic (NaOH) ethanol in the presence of hydroxy- and mercaptopyridine ligands (see Schemes 1 and 2, respectively).²⁵ The residual NaCl and the excess NaOH can be easily removed by drying the reaction mixture in vacuo, adding CH₂Cl₂, and filtering the solution. Presumably, the acidic OH and SH protons are removed by the base followed by nucleophilic displacement of the chloride at the metal center, generating

(18) Beurskens, P. T.; Admiraal, G.; Beurskens, G.; Bosman, W. P.; Garcia-Granda, S.; Gould, R. O.; Smits, J. M. M.; Smykalla, C. *The DIRDIF99 Program System*; Technical Report of the Crystallography Laboratory; University of Nijmegen: Nijmegen, The Netherlands, 1999.

(19) Sheldrick, G. M. *SHELXL-97, Programs for Crystal Structure Refinement*; University of Göttingen: Germany, 1997.

(20) Duisenberg, A. J. M.; Kroon-Batenburg, L. M. J.; Schreurs, A. M. *J. Appl. Crystallogr.* **2003**, *36*, 220–229.

(21) Herbst-Irmer, R.; Sheldrick, G. M. *Acta Crystallogr., Sect. B* **1998**, *54*, 443–449.

(22) Spek, A. L. *J. Appl. Crystallogr.* **2003**, *36*, 7.

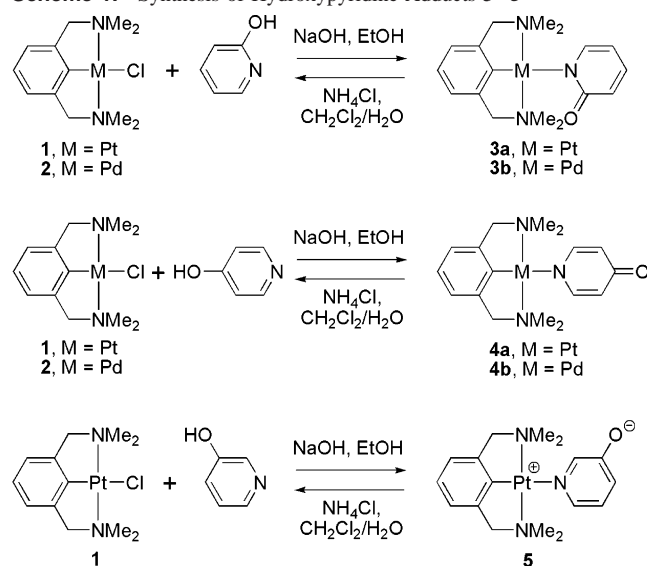
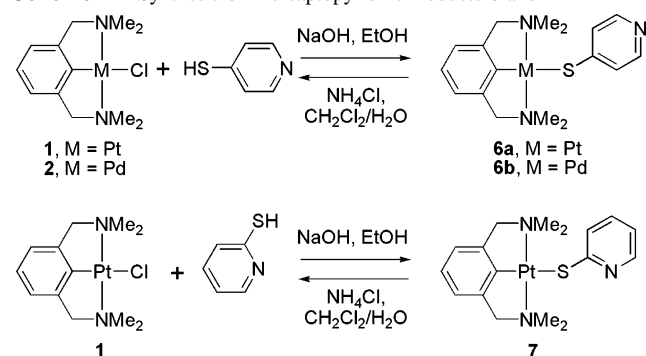
(23) Sheldrick, G. M. *SADABS—Bruker Nonius Area Detector Scaling and Absorption Correction*; University of Göttingen: Göttingen, Germany, 2002.

(24) Blessing, R. H. *Acta Crystallogr., Sect. A* **1995**, *51*, 33–38.

(25) *m*-Mercaptopyridine is not commercially available and is thus not studied here.

Table 2. Experimental Crystallographic Details for **6a**, **6b**, and **7**

	6a	6b	7
formula	C ₁₇ H ₂₃ N ₃ PtS	C ₁₇ H ₂₃ N ₃ PdS	C ₁₇ H ₂₃ N ₃ PtS
fw	496.53	407.84	496.53
cryst color	yellow	colorless	yellow
cryst size (mm ³)	0.30 × 0.21 × 0.18	0.30 × 0.06 × 0.06	0.60 × 0.21 × 0.12
cryst syst	triclinic	triclinic	monoclinic
space group	<i>P</i> 1̄ (no. 2)	<i>P</i> 1̄ (no. 2)	<i>P</i> 2 ₁ / <i>c</i> (no. 14)
<i>a</i> (Å)	9.3387(11)	9.308(3)	9.5326(3)
<i>b</i> (Å)	9.7915(9)	9.759(4)	10.0782(7)
<i>c</i> (Å)	10.4295(12)	10.5346(15)	17.4735(10)
α (deg)	114.871(8)	114.50(3)	90
β (deg)	95.018(11)	95.17(2)	96.076(4)
γ (deg)	95.766(9)	96.530(19)	90
<i>V</i> (Å ³)	851.91(16)	855.1(5)	1669.27(16)
<i>Z</i>	2	2	4
<i>D</i> _{calcd} (g/cm ³)	1.936	1.584	1.976
μ (mm ⁻¹)	8.358	1.207	8.531
abs corr	ABST (PLATON ²²)	none	SORTAV ²⁴
abs corr range	0.14–0.39		0.14–0.36
(sin θ/λ) _{max} (Å ⁻¹)	0.53	0.65	0.65
no. of measured reflns	12235	23600	27884
no. of unique reflns	2082	6900	3814
params/restraints	204/0	204/0	203/0
R1/wR2 [<i>I</i> > 2σ(<i>I</i>)]	0.0343/0.0971	0.0343/0.0805	0.0215/0.0482
R1/wR2 (all reflns)	0.0348/0.0975	0.0455/0.0846	0.0262/0.0501
<i>S</i>	1.137	1.114	1.131
ρ _{min} /max (e Å ⁻³)	−1.43/1.29	−0.65/0.82	−1.40/1.80

Scheme 1. Synthesis of Hydroxypyridine Adducts **3–5****Scheme 2.** Synthesis of Mercaptopyridine Adducts **6** and **7**

formally neutral NCN–M–py complexes (py = substituted pyridine); however, the initial coordination of the pyridine ligand to generate a charge-separated species cannot be ruled out. Like most other neutral Pt and Pd pincer compounds,^{1a}

the hydroxypyridone complexes are stable to air and atmospheric moisture in the solid state and in solution. Reaction of palladium pincer **2** with *m*-hydroxypyridine resulted in a black reaction mixture that could not be characterized. The mercaptopyridine adducts are somewhat less robust and exhibit decomposition in the air, possibly due to oxidation of the metal–sulfide group. Because of the strong, covalent M–N or M–S bonds (in the case of the ortho- and para-substituted systems) and the fact that the complexes are formally neutral, these species are resistant to reaction with the byproduct NaCl, and >95% yields of the Pt complexes are found. Most cationic NCN–Pt or NCN–Pd complexes containing neutral Lewis bases, such as pyridine, MeCN, or H₂O, can be smoothly converted to the respective halides by reaction with alkali metal halide salts, such as LiCl.¹ However, yields of the Pd complexes all hover at about 50%, perhaps indicating some back reaction with NaCl in addition to the other observed ill-defined decomposition processes. Pincers **1** and **2** can be quantitatively regenerated from complexes **3–7** by treatment with NH₄Cl in a biphasic CH₂Cl₂/H₂O system with release of the hydroxy- or mercaptopyridine ligand.

X-ray Crystallographic Studies. Hydroxypyridine Complexes. As there are two potential coordination sites available in the substituted pyridine ligands via N or O, the bonding mode of the ligand may be altered with changes in the regiochemistry of the heteroatoms. Obviously, this will have a great impact on subsequent reactivity. While both the ¹H and ¹³C NMR spectra of the complexes give an indication of the binding atom, X-ray crystallographic structural determination was necessary to unequivocally assign the geometry of the coordinated pyridine ligand. Notably, all the NMR data for **3–7** agree with the pyridine bonding mode found in the solid state, suggesting that these structures are also retained in solution. In **3** and **4** particularly, ¹H NMR signals are observed at 6.1–6.5 ppm that are diagnostic for nonaromatic pyridone-type structures, which are absent in the NMR spectra of complexes **5–7** containing the pyridine bonding mode. As shown in Scheme 1, reaction of NCN–PtCl (**1**) or NCN–PdCl (**2**) with *o*-, *m*-, or *p*-hydroxypyridines generates the N-bound complexes exclusively. Selected metrical data for **3–4** can be found in Table 3. For both Pt and Pd complexes of type **3** and **4**, which have *o*- and *p*-hydroxypyridine ligands, respectively, the observed bound ligand is the pyridone tautomer. For example, in the CH₂Cl₂ solvate of Pt complex **3a** with an ortho-substituted pyridone, the C13–O1 bond length is 1.255(4) Å, in line with a C=O double bond (see Figure 1). In addition, there is an alternation of long (C13–C14 = 1.435(5) and C15–C16 = 1.387(5) Å) and short (C14–C15 = 1.366(5) and C16–C17 = 1.365(5) Å) distances of the formal single and double bonds in the pyridone ring. Supporting evidence in solution is found in the ¹³C NMR spectrum, in which the C=O resonance appears in the normal range for a ketone at δ 171.4.

In the analogous structure of solvent-free Pd pincer **3b**, shown in Figure 2, a C13–O1 bond length of 1.251(3) Å is observed in addition to the same bond-length alternation

Table 3. Selected Bond Lengths (Å) and Angles (deg) for Hydroxypyridine Adducts 3–4

	3a	4a	3b	4b-1	4b-2
M–C	1.926(4)	1.932(5)	1.9200(18)	1.9146(17)	1.9180(17)
M–N (pincer)	2.079(3)	2.088(4)	2.0968(15)	2.1008(14)	2.1012(14)
	2.087(3)	2.089(4)	2.0970(16)	2.1042(14)	2.1047(14)
M–N (py)	2.137(3)	2.133(4)	2.1610(16)	2.1459(15)	2.1410(15)
C–O	1.255(4)	1.274(6)	1.251(3)	1.275(2)	1.285(2)
C–M–N (py)	178.72(13)	177.87(19)	179.34(7)	178.20(6)	178.27(7)
C–M–N (pincer)	82.44(14)	83.5(2)	81.99(7)	81.46(6)	81.61(7)
	81.68(14)	82.4(2)	82.53(7)	81.17(6)	81.40(7)
twist ^a	86.44(19)	85.2(2)	86.04(11)	77.60(8)	67.30(9)
out of plane ^b	C7 0.569(4)	C7 0.268(6)	C7 0.360(2)	C71 0.5855(18)	C72 0.5501(18)
	C10 –0.560(4)	C10 0.313(6)	C10a 0.229(3)	C101 –0.6455(17)	C102 –0.5908(18)
			C10b –0.538(17)		

^a Angle between the least-squares planes of the pyridine and pincer arene rings. ^b Distance the benzylic carbons are displaced out of the least-squares plane defined by the metal center, *ipso* carbon of the pincer arene, N atom of the amino groups, and pyridine/pyridone N. The relative sign of the values is arbitrarily assigned.

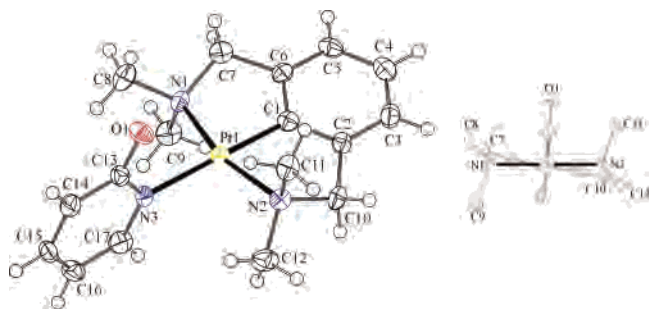


Figure 1. View of the molecular structure of **3a**. Displacement ellipsoids are drawn at the 50% probability level, and the cocrystallized CH₂Cl₂ solvent molecule has been removed for clarity. The inset shows a view along the N3–Pt1–C1 axis.

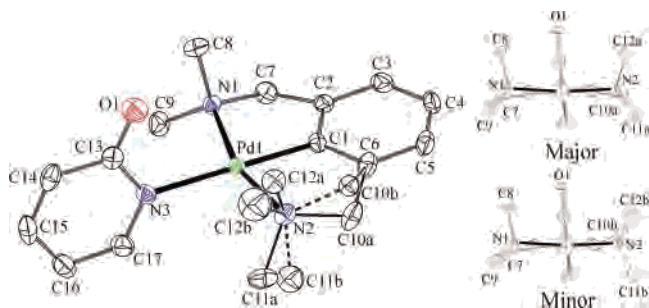


Figure 2. View of the molecular structure of **3b** with minor disorder component C10b, C11b, and C12b (10% occupancy) included; hydrogen atoms are removed for clarity. Displacement ellipsoids are drawn at the 50% probability level. The inset shows a view along the N3–Pd1–C1 axis.

(long: C13–C14 = 1.449(3), C15–C16 = 1.399(3) Å; short: C14–C15 = 1.360(3), C16–C17 = 1.365(3) Å) of the C–C linkages around the pyridone ring. In solution, the C=O peak occurs at δ 171.9 in the ¹³C NMR spectrum. Of particular note is that the major disorder component (90% occupancy) exhibits a rather peculiar configuration of the pincer ligand in complexes with a four-coordinate, square planar metal center.¹ In this structure, both of the benzylic carbons (C7 and C10a) are found on the same side of the plane of the pincer arene, which places the NMe₂ groups in an approximately eclipsed geometry (see inset of Figure 2, major isomer). In general, the benzylic carbons are found on opposite sides of the pincer arene ring, as this gives a sterically more favorable mutually staggered configuration of the groups on the ligated amines (see inset of Figure 1 and minor isomer of Figure 2). The benzylic protons C7 and

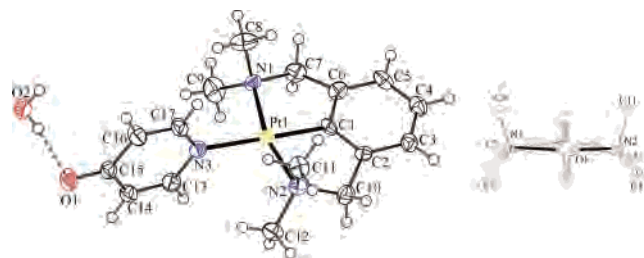


Figure 3. View of the molecular structure of **4a** with cocrystallized H₂O. Displacement ellipsoids are drawn at the 50% probability level. The inset shows a view along the N3–Pt1–C1 axis.

C10a are displaced to the same side of the plane formed by the square planar core of the complex, by 0.360(2) and 0.229(3) Å, respectively; the least squares plane contains atoms Pd1, C1, N1, N2, and N3. The minor disorder component exhibits the normally observed geometry and the benzylic carbon C10b is found 0.538(17) Å from the square planar core, opposite to C7.

Similar supporting evidence for pyridone tautomers are noted for the para-substituted complexes **4**. In the monohydrated Pt species **4a** (see Figure 3), the C15–O1 bond length is 1.274(6) Å, in line with a C=O double bond, and formal single (C14–C15 = 1.415(7), C15–C16 = 1.431(7) Å) C–C bonds are found. In addition, the somewhat unusual configuration of the major disorder component of the NCN ligand in **3b** is mirrored in **4a**. The benzylic carbons C7 and C10 are located on the same side of the pincer arene and displaced by 0.268(6) and 0.313(6) Å, respectively, from the Pt-centered square planar core of the complex. The Pd complex **4b**, shown in Figure 4, crystallizes with two independent molecules of **4b** and five water molecules in the asymmetric unit. In one (**4b-1**), the pyridone is coordinated symmetrically within the N–Pd–N pocket (Pd1–N31–O1 = 178.23(11)°), whereas the other (**4b-2**) exhibits a decidedly tipped orientation of the pyridone ligand toward one side of the N–Pd–N vector (Pd2–N32–O2 = 165.95(7)°). Other metrical parameters between the two molecules are very similar. The C–O bond lengths of C151–O1 = 1.275(2) and C152–O2 = 1.285(2) Å are found in **4b-1** and **4b-2**, respectively. For molecule **4b-1**, the bond-length alternation is again found within the pyridone ring; bond lengths for C141–C151 = 1.424(2) and C151–C161 =

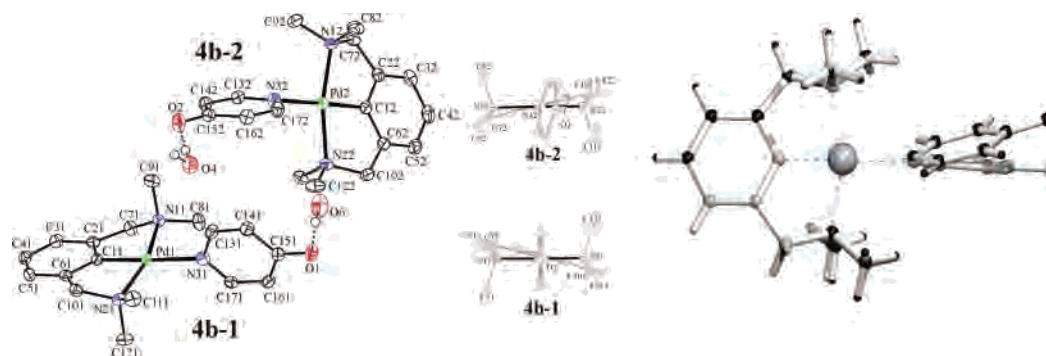


Figure 4. Left: View of the molecular structure of **4b**. Displacement ellipsoids are drawn at the 50% probability level; all C–H hydrogen atoms as well as three of the five cocrystallized H₂O molecules were deleted for clarity. The inset shows views along the N32–Pd2–C12 (**4b-2**) and N31–Pd1–C11 (**4b-1**) axis, respectively. Right: Quaternion fit²² of the two independent molecules in the crystal structure of **4b**. Water molecules are omitted in the fitting. Gray scale atoms depict **4b-1** and black atoms depict **4b-2**.

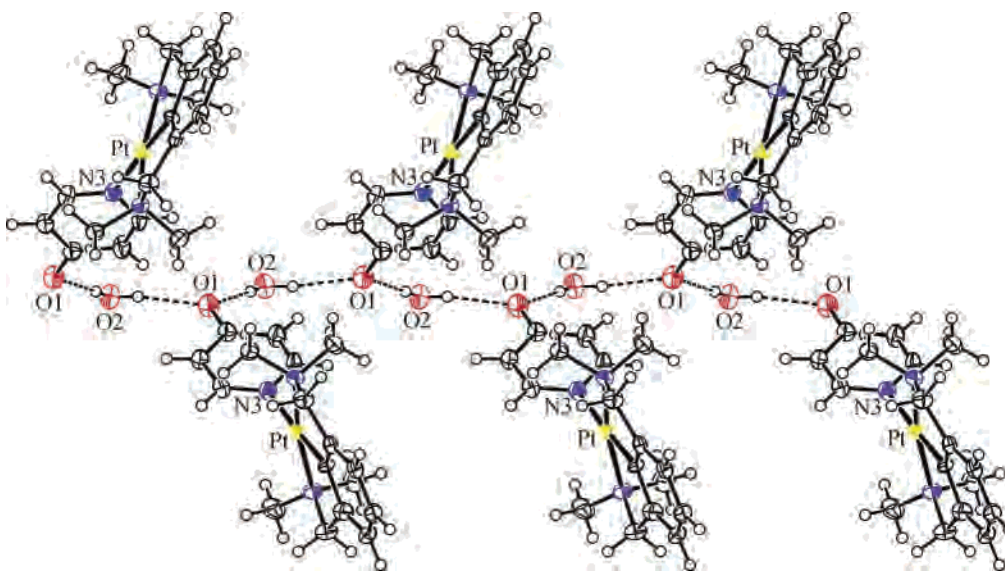


Figure 5. View of the *a,b*-face of the network hydrogen bonding in **4a**. Displacement ellipsoids are drawn at the 50% probability level.

1.427(2) Å for the long and C131–C141 = 1.365(3) and C161–C171 = 1.388(2) Å for the short linkages are noted. Similar variations are found in **4b-2**.

The limited number of other crystallographically characterized cationic NCN–Pt pyridine complexes exhibit somewhat longer Pt–pyridine bonds than observed for **3** and **4**, further indicating that the pyridone tautomer with a covalent M–N linkage dominates the bonding picture. A number of piperidyl NCN–Pt complexes incorporating substituted and bifunctional pyridine ligands exhibit Pt–pyridine distances ranging from 2.164(4) to 2.143(3) Å.²⁶ Somewhat more closely related dimethyl amino NCN–Pt–pyridine adducts exhibit Pt–pyridine bond lengths between 2.185(5) and 2.194(4) Å.^{14c,d}

Extensive hydrogen bonding between the *p*-pyridone O and cocrystallized water is also observed in the crystals of both **4a** and **4b**. In **4a**, a single water is found per pincer–pyridine unit. The water molecule is symmetrically bridging two pincer–pyridones with intermolecular O···H bonds of 2.00(5) and 2.03(5) Å. The hydrogen bonding forms a 1D

linear chain along the crystallographic *c*-axis (see Figure 5). In **4b**, five well-refined water molecules are found within the asymmetric unit. The water molecules containing O6 and O4 are hydrogen bonded to O1 and O2, respectively, of the two distinct pyridones. H···O bond lengths of 1.787(19) and 1.718(17) Å for O1–H(6B) and O2(H4B), respectively, are noted. The other three water molecules form a cluster of hydrogen bonds with each other, and O5 and O7 link this cluster to the next via interaction with O1 and O2, respectively (O1–H(5B) = 1.813(15) and O2–H(H7B) = 1.808(13) Å). This network forms a two-dimensional sheet in the crystallographic *a,b*-plane, as shown in Figure 6.

All other parameters for the binding of the pyridone and NCN pincer ligands to the metal center are very similar across complexes **3** and **4** (see Table 3.) The metal centers are in a distorted square planar geometry with slightly compressed C_{ipso}–M–N(pincer) angles ranging from 81.17(6) to 83.54(19)°. This is due to steric constraints imposed by the pincer ligand and is normally observed in square planar pincer complexes of this type. Also, the arene pincer and pyridone rings are almost orthogonal; the twist angle between the least squares planes of the two rings are 86.44(19), 86.04(11), and 85.2(2)° for **3a**, **3b**, and **4a**, respectively.

(26) (a) Jude, H.; Krause Bauer, J. A.; Connick, W. B. *Inorg. Chem.* **2005**, *44*, 1211. (b) Jude, H.; Krause Bauer, J. A.; Connick, W. B. *Inorg. Chem.* **2004**, *43*, 725.

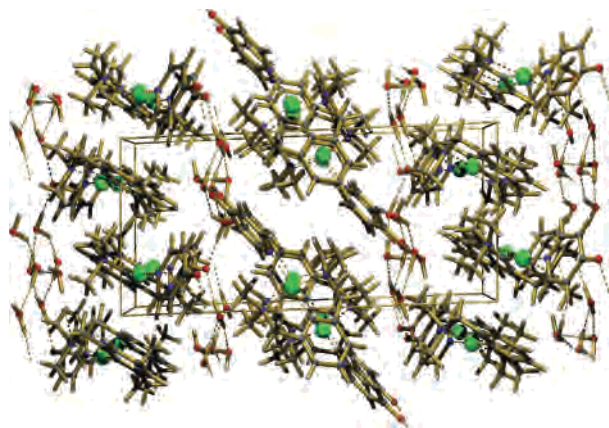


Figure 6. POV-RAY trace of the *a,c*-face of the hydrogen bond network in **4b**.

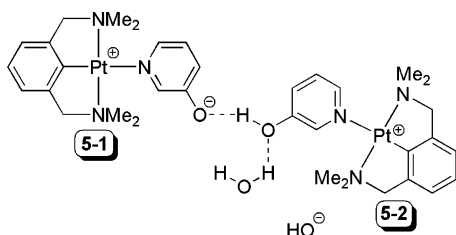


Figure 7. Depiction of the atom connectivity of **5** found in the crystal.

These twist angles in **4b** are slightly more compressed at 77.60(8) and 67.30(9)° for **4b-1** and **4b-2**, respectively, likely as a result of the extensive H-bonding network.

In the case of the *m*-hydroxypyridine ligand, tautomerization to a pyridone structure is not possible. Somewhat surprisingly, the Pt complex **5** still exhibits coordination of the pyridine through the neutral N atom. However, there were problems with the solution of the crystallographic data set. As shown in Figure 7, the structure indicated that both a zwitterionic pincer metal complex (**5-1**) and a cationic pincer species with a hydroxypyridine ligand (**5-2**) cocrystallize. The additional proton is presumed to originate from abstraction from the crystallization solvent (wet 2-propanol), and the charge balancing anion is likely a hydroxide that is extensively hydrogen bonded to water and 2-propanol within the solvent-filled voids. However, this anion could not be located with certainty, and due to the inability to locate and identify the co-anion in the structure, we feel that it is inappropriate to report the entirety of the structure. However, the data do give good evidence for the atom connectivity depicted. It should be stressed that the bridged structure indicated from the crystal data is only observed in the solid state and that the NMR spectra in solution are consistent with a monomeric species and an N-bound adduct in protic solvents (see below). The ¹³C NMR chemical shift for the C=O group of **5** in CD₃OD is shifted somewhat upfield (δ 167.1) compared to either **3** or **4**, suggesting less C=O character.

The difference in tautomer form between neutral pyridone or zwitterionic pyridine species has a distinct impact on the properties of the respective complexes. For example, complexes **3** and **4** are quite soluble in polar organic solvents such as CH₂Cl₂ or CHCl₃. On the other hand, **5** is highly

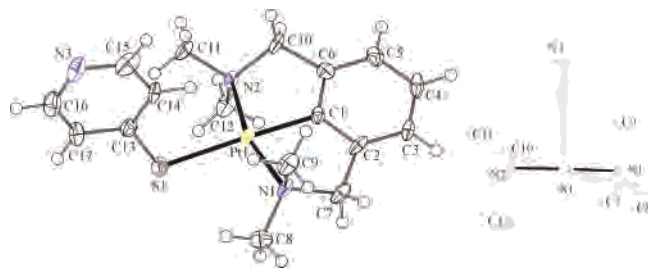


Figure 8. View of the molecular structure of **6a**. Displacement ellipsoids are drawn at the 50% probability level. The inset shows a view along the S1–Pt1–C1 axis.

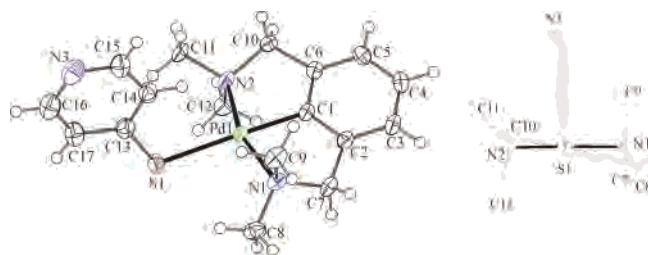


Figure 9. View of the molecular structure of **6b**. Displacement ellipsoids are drawn at the 50% probability level. The inset shows a view along the S1–Pd1–C1 axis.

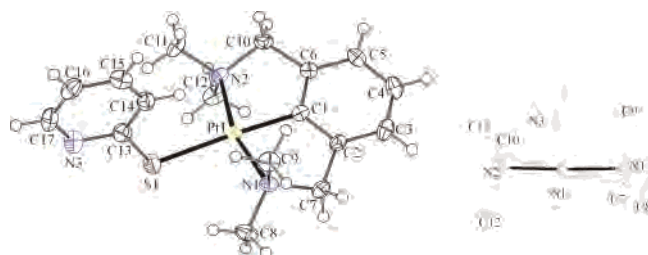


Figure 10. View of the molecular structure of **7**. Displacement ellipsoids are drawn at the 50% probability level. The inset shows a view along the S1–Pt1–C1 axis.

soluble in polar protic solvents, such as ethanol and methanol, but has limited solubility in other nonprotic organic solvents. In the ¹H NMR spectrum in CD₃OD, only one set of signals is observed and is consistent with the N-bound complex. In CD₂Cl₂ or CDCl₃, small amounts of additional signals are found in the aromatic region, tentatively pointing to the possible presence of O-bound structures in aprotic solutions in which the anionic oxygen cannot be stabilized by hydrogen bonding with the solvent. Unfortunately, attempts to obtain X-ray quality crystals of **5** from aprotic solvents have been unsuccessful to date.

X-ray Crystallographic Studies. Mercaptopyridine Complexes. In contrast to the preferred N-coordination observed for the hydroxypyridine complexes, sulfur containing *o*- and *p*-mercaptopyridines were found to coordinate exclusively through the sulfur atom (see Scheme 2). These are, to the best of our knowledge, the first examples of crystallographically characterized pincer-supported terminal thiolate complexes of Pt and Pd. In accord with neutral pyridone complexes **3** and **4**, thiolate bound pincer complexes **6** and **7** are highly soluble in CH₂Cl₂. Additionally, Pt complex **6a** and Pd complex **6b** are isostructural in the solid state. Views of the molecular structures are given in Figures 8–10, and selected bond lengths and angles are given in Table 4.

Table 4. Selected Bond Lengths (Å) and Angles (deg) for Mercaptopyrindine Adducts **6a** and **7**

	6a	7	6b
M–C	1.947(11)	1.928(4)	1.931(3)
M–N (pincer)	2.094(9)	2.100(3)	2.112(2)
	2.107(8)	2.095(3)	2.111(2)
M–S	2.426(3)	2.4040(10)	2.4516(13)
C–S	1.758(11)	1.742(4)	1.741(3)
C–M–S	176.9(3)	173.49(11)	176.90(8)
C–S–M	109.7(4)	107.60(15)	109.86(10)
C–M–N (pincer)	81.4(4)	81.36(14)	81.08(10)
	81.8(4)	82.20(14)	80.97(10)
twist ^a	78.7(6)	82.48(19)	79.03(14)
out of plane ^b	C7 –0.596(11)	C7 –0.609(4)	C7 –0.604(3)
	C10 0.494(11)	C10 0.476(4)	C10 0.512(3)

^a Angle between the least-squares planes of the pyridine and pincer arene rings. ^b Distance the benzylic carbons are displaced out of the least-squares plane defined by the metal center, *ipso* carbon of the pincer arene, N atoms of the amino groups, and thiolate S. The relative sign of the values is arbitrarily assigned.

A search of the Cambridge Structural Database²⁷ reveals that mutual trans orientation of a thiolate to alkyl, aryl, or alkene ligands in Pt or Pd complexes is relatively rare. Pt complexes with *p*- (**6a**) and *o*-mercaptopyridine (**7**) have Pt–S bonds of 2.426(3) and 2.4040(10) Å, respectively, which are somewhat longer than those in other related Pt thiolate complexes. Pt–S bonds of 2.287(3)–2.344(1) Å are found for a limited selection of pertinent species.²⁸ Analysis of Pd–S bond lengths shows that the bond in **6b** (Pd1–S1 = 2.4516(13) Å) is also relatively long compared to structurally related complexes (range 2.339–2.391 Å).²⁹ This elongation is likely due to the strong trans-influence of the pincer aryl anion. In **6a**, the Pt–S–C angle is decidedly bent at 109.7(4)°, in accord with other metal–sulfide complexes. The C–S bond length (1.758(11) Å) is also in the normal range for a C–S single bond. Analogous bond lengths and angles for **6b** and *o*-mercaptopyridine complex **7** are quite similar to those for **6a** (see Table 4). In accord with complexes **3** and **4**, the metal centers in **6** and **7** are in distorted square planar environments with slightly compressed C–M–N angles (range 80.98(11)–82.20(14)°). As the pyridine ring is not directly bound to the metal, the angle between the pincer arene and pyridine rings (78.7(6) to 82.48(19)°) is slightly larger than those found in **3** and **4**, with the exception of **4b**. The free pyridine N has no close contacts with other functionalities in the solid state and is essentially a free Lewis base with the closest contacts found to the protons of the pyridine ring in adjacent molecules at distances between 2.69 and 2.87 Å. In addition, the NCN pincer ligands are all bound in the more common configuration with staggered NMe₂ groups and benzylic carbons on opposite sides of the pincer arene plane.

(27) Allen, F. H. *Acta Cryst.* **2002**, *B58*, 380–388.

(28) (a) Cooper, M. K.; Hair, N. J.; Yaniuk, D. W. *J. Organomet. Chem.* **1978**, *150*, 157. (b) Howard, W. A.; Bergman, R. G. *Polyhedron* **1998**, *17*, 803. (c) Osakada, K.; Hosoda, T.; Yamamoto, T. *Bull. Chem. Soc. Jpn.* **2000**, *73*, 923.

(29) (a) Schreiner, B.; Urban, R.; Zografidis, A.; Sunkel, K.; Polborn, K.; Beck, W. *Z. Naturforsch., B: Chem. Sci.* **1999**, *54*, 970. (b) Osakada, K.; Ozawa, Y.; Yamamoto, A. *Bull. Chem. Soc. Jpn.* **1991**, *64*, 2002.

Conclusions

A silver-free and chemically reversible route for halide abstraction and ligation of various hydroxy- and mercaptopyrindine complexes in NCN–Pt and NCN–Pd species has been reported using basic ethanol as the solvent. On the basis of X-ray crystallographic studies, the binding mode of the substituted pyridine ligand is dependent on the type of heteroatoms present. In the case of hydroxypyridines, binding to the metal centers is found exclusively through the N-center. In the *o*- and *p*-hydroxypyridine, the ligand tautomerizes to the pyridone form, and a formally covalent N–M bond is generated. The coordination mode of *m*-hydroxypyridine is somewhat more complex, as tautomerization is not possible. In polar, aprotic solvents, such as CD₂Cl₂, there is tentative evidence for competition between the zwitterionic N-bound and neutral O-bound modes by ¹H NMR experiments. In protic solvents, such as CD₃OD, the N-bound mode dominates, either due to stabilization of the oxypyridine by H-bonding or abstraction of a proton from the solvent, generating an ion pair. Crystal structure evidence points to the preference of the N-bound mode in the solid-state. In contrast, the mercaptopyrindine ligands coordinate exclusively via the S atom, generating the first examples of pincer thiolate complexes. This difference coordination mode is likely due to the softer coordinating nature of S vs O, which better matches with the soft Pt^{II} and Pd^{II} centers.³⁰

Recently, pincer–pyridine complexes have been employed in the context of materials chemistry in the detailed delineation of thermodynamic vs kinetic effects in the assembly of main-chain reversible polymers and as cross-linkers in supramolecular networks.¹¹ The compounds reported here may be potentially useful in further extensions of this work. The bonding between *o*- and *p*-hydroxy- and mercaptopyrindines and the metal centers is covalent, which removes any potential complexity introduced by counterions, and the interaction is generally stronger than the typical dative ligation of pyridine ligands. As the directionality and strength of interactions between the individual units determine the shapes of the supramolecules, which, in turn, govern their bulk properties,³¹ the studies here point to the possible use of hydroxy- and, to a lesser extent because of their lower stability, mercaptopyrindine-ligated pincer complexes in this context. Also, as the reaction is chemically reversible by addition of NH₄Cl, chemically controlled covalent assembly/disassembly of networks can be envisioned. A recent example of noncovalent, reversible, chemically controlled assembly/disassembly of a metal-containing dendrimer via Pd–pyridine interactions³² highlights the potential use of this

(30) Pearson, R. G. *Hard and Soft Acids and Bases*; Dowden, Hutchinson and Ross: Strousbourg, PA, 1973.

(31) (a) Lehn, J.-M. *Supramolecular Chemistry: Concepts and Perspectives*; Wiley-VCH: Weinheim, Germany, 1995. (b) Whitesides, G. M.; Mathias, J. P.; Seto, C. T. *Science* **1991**, *254*, 1312. (c) Lehn, J.-M. *Chem.–Eur. J.* **1999**, *5*, 2455. (d) Brunsveld, L.; Folmer, B. J. B.; Meijer, E. W.; Sijbesma, R. P. *Chem. Rev.* **2001**, *101*, 4071. (e) Davis, A. V.; Yeh, R. M.; Raymond, K. N. *Proc. Natl. Acad. Sci. U.S.A.* **2002**, *99*, 4793.

(32) Onitsuka, K.; Iuchi, A.; Fugimoto, M.; Takahashi, S. *Chem. Commun.* **2001**, 741.

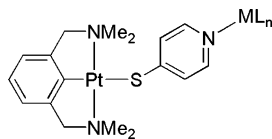


Figure 11. Example of a mixed-metal heteroleptic complex.

type of methodology. Further, the pyridine ring in the NCN–M thiolate systems is free for subsequent reactivity, and the generation of mixed-metal heteroleptic complexes (see Figure 11) is also a possibility. Studies exploring these aspects of this chemistry are ongoing.

Acknowledgment. This research was supported by The Netherlands Research School Combination Catalysis (NRSC-C, A.V.C.), the Natural Sciences and Engineering Research Council of Canada (P.A.C.), jointly by the NWO (Netherlands) and RFBR (Russia), International Grant 047.015.005, and in part by the Council for Chemical Sciences of The Netherlands Organization for Scientific Research (CW-NWO, A.M.M., M.L., and A.L.S.).

Supporting Information Available: CIF files for compounds **3a**, **3b**, **4a**, **4b**, **6a**, **6b**, and **7**. This material is available free of charge via the Internet at <http://pubs.acs.org>.

IC051773X